Monte Carlo study of the antiferromagnetic two-dimensional Blume-Capel model

J. D. Kimel, S. Black, P. Carter, and Yung-Li Wang
Department of Physics, Florida State University, Tallahassee, Florida 32306
(Received 11 August 1986)

A Monte Carlo simulation is used to investigate the two-dimensional spin-1 Ising antiferromagnet in the presence of an external magnetic field and a single-ion potential. Comparison is made between the results of this simulation and previous mean-field calculations. The phase diagram and the critical behavior of the model are discussed. In contrast to the mean-field picture, no decomposition of the tricritical point is observed.

I. INTRODUCTION

The spin-1 Ising antiferromagnet with zero-field splitting,[1] i.e., the antiferromagnetic Blume-Capel model,[2,3] has an unusually rich phase diagram, especially in the presence of an external magnetic field.[1] The model includes, in addition to a spin-1 Ising-like exchange interaction among nearest-neighbor pairs, an interaction with an external magnetic field H as well as a single-ion potential proportional to Δ, which yields a singlet ground state. Considerable progress has been made in understanding this model. Along the $H=\Delta=0$ line a second-order phase transition takes place between the antiferromagnetic staggered phase and the disordered phase, and a low-temperature (T) series expansion[4] has been developed and used to estimate the critical temperature T_c. The phase diagram in the Δ-T plane consists of a line of second-order critical points which ends and goes over to a first-order transition line at the tricritical point. Tricritical indices for the model in two lattice dimensions have been determined by Landau and Swendsen[5] on the basis of Monte Carlo renormalization-group studies.

Using the mean-field approximation, Wang and Rauchwarger[1] have shown that for $H\neq 0$ the tricritical point decomposes into a critical end point and a double critical point for a range of values of Δ. A thorough investigation of this feature in a two-dimensional lattice by Monte Carlo simulation, an approach which includes the correlated fluctuations ignored by the mean-field approximation, is a central outcome of the present work.

In this paper we present the results of a Monte Carlo simulation of the antiferromagnetic Blume-Capel model on a two-dimensional lattice. The code for this simulation is highly vectorized to run on the Florida State University CDC CYBER 205 and achieved a rate of 1.5×10^6 spin updates per second. The objectives of this simulation are (i) to determine the phase diagram in the T-H-Δ parameter space, (ii) to obtain the tricritical line as it evolves away from the $H=0$ plane, and (iii) to investigate the existence of the decomposition of the tricritical point predicted by the mean-field approximation. Furthermore as a by-product we use finite-size scaling to determine T_c for $\Delta=H=0$ with a very high accuracy. Our paper is organized as follows. In Sec. II we describe the antiferromagnetic Blume-Capel model and briefly outline the formalism of the Monte Carlo approach we used in the simulation. In Sec. III we present the results of our simulation and in Sec. IV we compare our results with previous calculations and draw our conclusions.

II. THE MODEL AND MONTE CARLO SIMULATION

The Hamiltonian for the antiferromagnetic Blume-Capel model is given by[1]

$$\mathcal{H}=J\sum_{nn} s_i s_j+\Delta\sum_i s_i^2-H\sum_i s_i \ , \tag{2.1}$$

where the antiferromagnetic coupling J acts only between nearest-neighbor pairs and s_i is the z component of the spin of the ith site and takes values $s_i=-1,0,1$. The second term in the Hamiltonian corresponds to the single-ion anisotropy and the last term represents the effects of an external longitudinal field. We restrict our study to positive Δ for which the critical behavior of the system includes first- as well as second-order phase transitions.

Our two-dimensional $L\times L$ square lattice contains $N=L^2$ spins, and we use the well-known Metropolis[6] algorithm with periodic boundary conditions to update the lattice configurations. The physical quantity O is then estimated by $\langle O\rangle$, where

$$\langle O\rangle=\sum_c O(c)/S \ , \tag{2.2}$$

and c runs over the configurations obtained by using the Metropolis algorithm to update the lattice over one sweep of the entire N spins of the lattice (one Monte Carlo step). Counted after the system reaches thermal equilibrium, S is the number of Monte Carlo steps (MCS). Since we are considering the antiferromagnetic coupling in Eq. (2.1), i.e., $J>0$, the relevant low-temperature order parameter is the staggered magnetization $\langle M\rangle$ and is estimated from Eq. (2.2) in which is used

$$M(c)=\sum_i \delta_i s_i(c)/N \ , \tag{2.3}$$

where i runs over the lattice sites and $\delta_i=+1$ (-1) for

even (odd) sites. Let us define (s_e, s_o) to be the ordered configuration at zero temperature in which the sublattice made up of even sites has $s_i = s_e$ and the sublattice of odd sites has $s_i = s_o$. Then the order parameter for the $(1,-1)$ configuration is $|M| \equiv \langle |M| \rangle$. Also of use will be the quadrupole moment $Q(c) = 1 - s^2(c)$, where

$$s^2(c) = \sum_i s_i^2(c)/N \ . \tag{2.4}$$

In order to measure phase boundaries we shall find useful the measurement of fluctuations in O defined by $(\Delta O)^2 = \langle O^2 \rangle - \langle O \rangle^2$. Thus the specific heat is

$$C_v = N(\Delta U)^2/(k_B T^2) \ , \tag{2.5}$$

where U is the energy per lattice site; the staggered magnetic susceptibility is

$$\chi_m = N(\langle M^2 \rangle - \langle M \rangle^2)/(k_B T) \ . \tag{2.6}$$

Because of the large fluctuations in χ_m due to the term $\langle M \rangle^2$ ($\langle M \rangle = 0$ for a finite lattice after a sufficient number of sweeps), we are also led to consider

$$\chi_{m0} = N\langle M^2 \rangle/(k_B T) \ , \tag{2.7}$$

and

$$\chi'_m = N(\langle M^2 \rangle - \langle |M| \rangle^2)/(k_B T) \ . \tag{2.8}$$

Peaks in the latter quantity we found useful in determining phase boundaries, particularly where the specific heat does not show a pronounced peaking behavior.

In treating errors we use the binning method for reliable error estimates.[7] If the S sweeps are binned into n equal binds of S_n sweeps each, then the average of a quantity O within a bin is

$$\langle O \rangle_b = \sum_{c \in \text{bin}} O(c)/S_n \ . \tag{2.9}$$

The mean value of O for the whole of the data is

$$\langle O \rangle = \sum_{\text{bins}} \langle O \rangle_b / n \ , \tag{2.10}$$

and the uncertainty estimate for $\langle O \rangle$, i.e., $\delta\langle O \rangle_n$, is

$$\delta\langle O \rangle_n = \left[\sum_{\text{bins}} (\langle O \rangle_b - \langle O \rangle)^2/n(n-1) \right]^{1/2} \ . \tag{2.11}$$

The naive estimate assuming each sweep corresponds to an uncorrelated configuration corresponds to $n = S$ and $S_n = 1$. However, as n is decreased, the estimate $\delta\langle O \rangle_n$ increases initially but then flattens out and becomes essentially independent of n. This yields a reliable estimate of the uncertainty in our measurements.

III. RESULTS

A. Phase diagram in T-H-Δ parameter space

The lattice-size dependence of our measurements of the magnetization, the specific heat, and the magnetic susceptibility is qualitatively similar to that observed elsewhere for similar systems and will not be presented here in detail. Rather we present first the qualitative picture of the phase diagram of the system in the space of T, H, and Δ. Also of interest is the phase diagram in the $\Delta = 0$ plane which we show in Fig. 1. Along the first-order line in this figure strong hysteresis was observed when crossing the first-order line in the Δ direction. The first-order line was determined using a mixed start technique[8] in which we initialize the upper half of the lattice to the $T = 0$ configuration expected on one side of the first-order boundary, i.e., $(1,-1)$, and initialize the lower half to the configuration on the other side of the first-order boundary, (0,0). With these initial conditions every update sweep of the lattice was monitored. If the system was on the antiferromagnetically ordered side of the first-order boundary, we observed after a relatively few sweeps (up to 50 000) that the order parameter $|M|$ became large (> 0.75), whereas if the system was on the other side of the first-order boundary, the order parameter for the (0,0) configuration, the quadrupole moment Q, was observed rapidly to become large (> 0.75). Using this technique, we measured the first-order line of Fig. 1 to a statistical accuracy of 1%. The second-order phase boundary was obtained from peaks in the specific heat and susceptibility. For $\Delta = 0$ and $H = 0$, T_c was obtained by the use of finite-size scaling and the assumption of universality of the critical exponents β and γ and will be discussed in detail later. The tricritical point was determined by finding the point where hysteresis starts in the measurement of the order parameter when crossing the phase boundary in the Δ direction. Further discussion of this point will be found later when we describe our measurement of the tricritical line with $H \neq 0$.

Figure 2 shows the phase diagram in the space of T, H, and Δ. The solid lines in the $T = 0$ plane exhibit the boundaries which separate the various configurations shown and were obtained from Eq. (2.1) using equality of the energies along the configuration boundaries. The data for the boundaries of the planes of constant Δ, i.e., $\Delta/J = 0$, 1, and 2.25, were obtained for a lattice of size

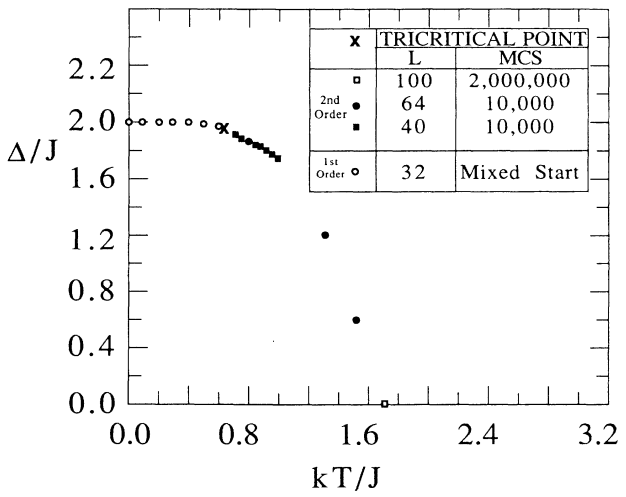

FIG. 1. Phase diagram for the antiferromagnetic Blume-Capel model in the $H = 0$ plane.

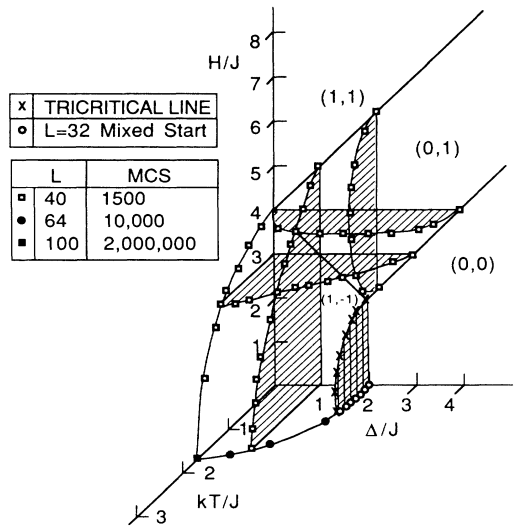

FIG. 2. Phase diagram for the antiferromagnetic Blume-Capel model in the parameter space of T, H, and Δ. The spin configurations of the lattice at $T=0$ are designated by (s_e,s_o).

$L=40$ and 1500 Monte Carlo steps after 500 sweeps had been discarded to allow the system to come to thermal equilibrium. After each boundary point was determined, the required series of measurements were repeated, incrementing the measurements in the opposite direction to look for hysteresis effects which might suggest a first-order transition. None was found. In this region of parameter space, the phase transitions showed up clearly in our data as peaks in the specific heat and susceptibility, and this allowed us to map out these boundaries with relatively few Monte Carlo steps. Similar measurements yielded the boundaries shown for the planes of constant H for $H/J=3$ and 4. The peaks in the magnetic susceptibility and specific heat at these boundaries were observed to grow with increasing lattice size as would be expected from finite-size scaling[9,10] for a second-order phase transition. The tricritical line nearly falls in the plane $\Delta/J=2$, and the first-order phase boundary is depicted by the cross-hatched area in Fig. 2.

B. Finite-size scaling, critical indices, determination of T_c

Finite-size scaling[9] has been reviewed elsewhere[10] and will be discussed here only briefly. Qualitative confirmation of finite-size scaling of Monte Carlo data has been obtained for a variety of Ising-like models, both for two- and three-dimensional lattices.[7,11-13] We too have verified the qualitative features predicted by finite-size scaling and find the second-order transition at $H=\Delta=0$ with $T_c\simeq 1.694$ consistent with the exactly known critical indices expected for the two-dimensional Ising-like universality[14] class, $\beta=0.125$,[15] $\gamma=1.75$,[16] and $\nu=1$.[17] With these values of the critical indices, we found that the $\chi L^{-\gamma/\nu}$ and $ML^{\beta/\nu}$ at different T and L then collapse onto universal curves in terms of the scaled variable $(T-T_c)L^{1/\nu}$. Qualitatively similar results have been found earlier.[7,11-13] We also have taken a series of three measurements radially across the second-order transition boundary shown in Fig. 1. The data were taken in the $(k_BT/J,\Delta/J)$ range along the boundary from (0.68,1.944) up to the tricritical point at (0.619,1.97). Fitting $|M|=A|(1-R_c/R)|^{\beta}$ and $\chi_m=B(1-R_c/R)^{-\gamma}$ with $R=[(k_BT/J)^2+(\Delta/J)^2]^{1/2}$, we find for $L=100$ and MCS equal to 15000 that the effective critical indices trend smoothly to $\beta_t=0.042\pm0.004$ and $\gamma_t=1.09\pm0.1$ consistent with the tricritical indices of Landau and Swendsen, $\beta_T=0.039$ and $\gamma_t=1.03$, who obtained their results[5] using a different approach, the Monte Carlo renormalization group.

But here we stress our effort to go beyond[18,19] a qualitative confirmation of finite-size scaling and to use finite-size scaling together with the assumption of universality[14] of the critical exponents β, γ, and ν to determine to high statistical accuracy T_c, the critical temperature for $\Delta=H=0$. This approach is similar to, but the reverse of, the method of Refs. 18 and 19, where finite-size scaling was used to determine γ for the three-dimensional Ising model with input of an independently determined value for T_c. On the basis of finite-size scaling we expect the lattice size dependence of the susceptibility and order parameter $|M|$ precisely at $T=T_c$ to be[9,10]

$$\chi_{m0}=AL^{\gamma/\nu}, \tag{3.1}$$

$$|M|=BL^{-\beta/\nu}. \tag{3.2}$$

However, away from T_c these dependences will be altered. In addition there are nonleading corrections to Eqs. (3.1) and (3.2) which can be seen as deviations from these relations for smaller L. Thus if we assume (i) that χ_{m0} and $|M|$ scale according to the finite-size scaling relations given by Eqs. (3.1) and (3.2) at $T=T_c$ and (ii) that universality holds for the critical exponents β and γ, we can then determine to a high statistical accuracy T_c by demanding that χ_{m0} and $|M|$ satisfy finite-size scaling at $T=T_c$.

The critical exponents are known exactly to be $\beta=\frac{1}{8}$, $\gamma=\frac{7}{4}$, and $\nu=1$ for the two-dimensional spin-$\frac{1}{2}$ Ising model.[17] We assume by universality that the same exponents are correct for the present spin-1 Ising model. A low-temperature series expansion calculation[4] gives $T_c=1.690(6)$, where in parentheses is shown the expected uncertainty in the last digit. Figure 3 shows our measurement of $\chi_{m0}L^{-1/75}$ and $|M|L^{+0.125}$. It should be pointed out that in order to test and use this aspect of finite-size scaling, runs with very high statistics are required. For $L<70$ we discarded 100000 sweeps of the lattice for thermalization and then measurements of physical quantities were made for each lattice sweep. For each $L<70$, 500000 sweeps of the lattice were made for each measured point in Fig. 3, whereas for $L\geq 70$, 100000 sweeps were discarded for lattice thermalization and data were taken for 2000000 lattice sweeps at each L to give the measured results for Fig. 3.

It should be clear that our measurements are not consistent with finite-size scaling for the *central* value (uncer-

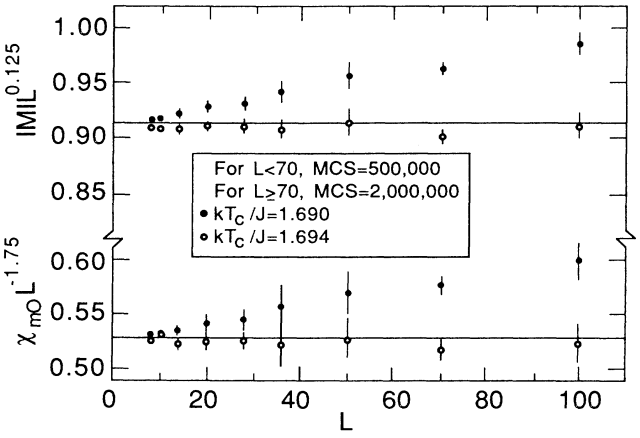

FIG. 3. Comparison of finite-size scaling with Monte Carlo measurements. The data would be horizontal to satisfy finite-size scaling exactly.

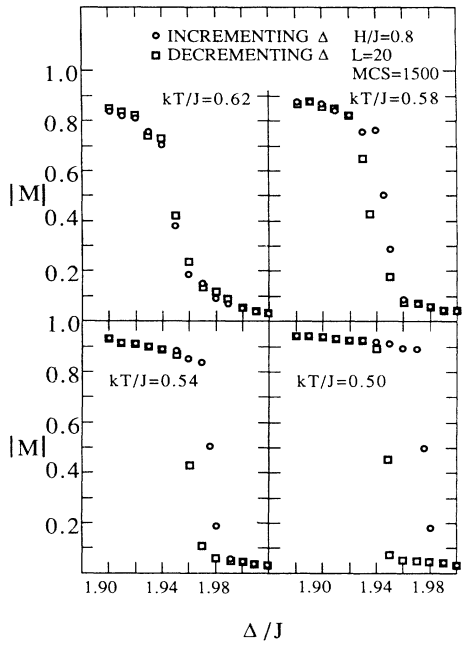

FIG. 4. Typical hysteresis observed in crossing the first-order transition boundary.

tainties in the series result will be discussed later) of the series-expansion calculation, $T_c=1.690$. Also our neglect of nonleading terms in Eqs. (3.1) and (3.2) cannot explain the discrepancy between our measurements and the horizontal line predicted by finite-size scaling since these corrections would show up at small L, not at large L where the discrepancies actually occur. From preliminary results we obtained, it is clear that χ_{m0} and $|M|$ fall faster for larger assumed values of T_c, so we also took measurements at $T=1.694$ and these results are also shown in Fig. 3. These measurements are consistent within our errors with the finite-size scaling relations (3.1) and (3.2) which hold at $T=T_c$, so we conclude that $T_c=1.694(2)$, where the uncertainty is estimated from Fig. 3. We also see that the change in T_c from the central value of the series expansion calculation required to be consistent with finite-size scaling, from 1.690 to 1.694 is within the quoted uncertainty of the series calculation. Thus the present technique yields a value for T_c consistent with the series expansion calculation but with reduced uncertainty in the result.

C. Determination of the tricritical line

The location of the tricritical line was determined using a combination of mixed start[8] results and observing the beginning of the onset of hysteresis in the measurement of the order parameter $|M|$ as the boundary of the first-order region is encountered from the second-order side. In the first set of measurements, we fixed H and made measurements of the order parameter first incrementing steps in Δ then decrementing steps in Δ to measure the hysteresis in $|M|$ for $T=T_i$. In the first-order region, strong evidence for hysteresis was apparent as shown in Fig. 4 for $H/J=0.8$ and $0.5\leq k_BT/J\leq 0.62$. For a given H and T the hysteresis was calculated as follows:

$$\xi=\sum_i[\,|M|_i(I)-|M|_i(D)]\,, \tag{3.3}$$

where i labels values of Δ and $|M|_i(I)$ is the order parameter at Δ_i, T, H obtained by incrementing Δ and $|M|_i(D)$ is obtained similarly by decrementing Δ. Thus Eq. (3.3) gives the area exhibited by the hysteresis plots of Fig. 4. The value of T on the critical line at this value of H was determined by fitting $\xi(T)$ as determined from Eq. (3.3) for various T_i as shown in Fig. 4 to

$$\xi(T)=A(T_t-T)^a \quad \text{for } T\leq T_t$$
$$=0 \quad \text{for } T>T_t\,. \tag{3.4}$$

It should be pointed out that we made the determination of T_t with measurements at much finer steps in T than is displayed in Fig. 4 where the choices of T_i were chosen to show the evolution of the hysteresis clearly. After T_t was determined, Δ_t was obtained using the mixed start approach by determining (for H fixed) the first-order phase boundary as a function of T and Δ. For $T=T_t$, the value of Δ which is on the first-order boundary is Δ_t. Similarly other points on the tricritical line at fixed T rather than fixed H were determined by reversing the rolls of T and H in the above procedure. The parameters for the tricritical line are summarized in Table I.

D. Nondecomposition of the tricritical point

One of the most interesting and elusive features of the antiferromagnetic Blume-Capel model in the presence of an external magnetic field which is predicted by mean-field theory is the decomposition of the tricritical point into a critical end point and a double critical point. Our investigation of this question constitutes the main results of this paper, which are summarized in Fig. 5.

TABLE I. The parameters of the tricritical line.

k_BT/J	H/J	Δ/J
$0.619^{\pm0.05}_{\pm0.02}$	0.0	1.97±0.02
$0.65^{\pm0.05}_{\pm0.02}$	0.4	1.95±0.03
$0.623^{\pm0.08}_{\pm0.03}$	0.8	1.95±0.04
$0.57^{\pm0.12}_{\pm0.06}$	1.2	1.96±0.05
$0.46^{\pm0.09}_{\pm0.04}$	1.6	1.95±0.02
0.35	$1.84^{\pm0.16}_{\pm0.14}$	1.971±0.012
0.2	$1.84^{\pm0.08}_{\pm0.05}$	1.983±0.008
0.05	$2.00^{\pm0.08}_{\pm0.05}$	2.000±0.004

For $H/J>2$, there is a broad region of second-order phase transition between the antiferromagnetically ordered (staggered) phase and the paramagnetic (disordered) phase. The points of this boundary were determined by observation of peaks in the magnetic susceptibility. Along the boundary the susceptibility and order parameter $|M|$ scaled with lattice size as expected,[9,10]

$$\chi_m(L')/\chi_m(L)=(L'/L)^{\gamma/\nu}, \tag{3.5}$$

$$|M|(L')/|M|(L)=(L'/L)^{-\beta/\nu}, \tag{3.6}$$

with $\beta=0.125$, $\gamma=1.75$, and $\nu=1$, characteristic of second-order critical indices of the two-dimensional Ising universality class. For $H/J<1.75$, the phase boundary is distinctly first order, and the first-order boundary points shown in Fig. 5 were determined from the mixed-start technique, described earlier, with $L=32$. In this region of H the first-order phase boundary exhibited a decided discontinuity in $|M|$ as well as the hysteresis one would expect of a first-order phase transition. Perhaps the best way to exhibit the distinct first-order character of the phase transition in this region is to display the metastability of the system along the boundary where the system remains in one of the metastable configurations and then quickly shifts to the other metastable configuration. This dramatic flipping between metastable states characteristic of a first-order phase transition boundary is shown in Fig. 6.

The region in parameter space where the phase boundary changes rapidly and where the nature of the phase transition changes is shown in the boxed region of Fig. 5. It is within this region where we have concentrated our efforts to clarify the question of the nature of the region's criticality. First consider the region at $k_BT/J\simeq0.19$, where the second-order boundary shows a large curvature and swings down toward the tricritical point. Figure 7 shows our measurements of the lattice-size dependence of the order parameter as a function of external magnetic field. In Fig. 7(a) at $k_BT/J=0.19$ the size dependence has virtually ceased, whereas in Fig. 7(b) at $k_BT/J=0.195$ the lattice-size dependence of $|M|$ is as expected for a second-order phase transition and suggests strongly second-order transitions both at $H/J\simeq1.85$ and $H/J\simeq1.97$. Similar measurements at $k_BT/J=0.18$ and $k_BT/J=0.17$ show no discernible size dependences of $|M|$ and the susceptibility. Thus $k_BT/J\simeq0.19$ represents the tip of the transition boundary.

At $k_BT/J=0.21$ we have made high-statistics measurements of the lattice-size dependence of $|M|$ in the region of the phase transition at $H/J\simeq1.81$, the results of which are shown in Fig. 8(a). This figure shows distinctly that (i) $|M|$ falls smoothly across the transition region and (ii) the size dependence expected of a second-order phase transition is exhibited. These two pieces of evidence sug-

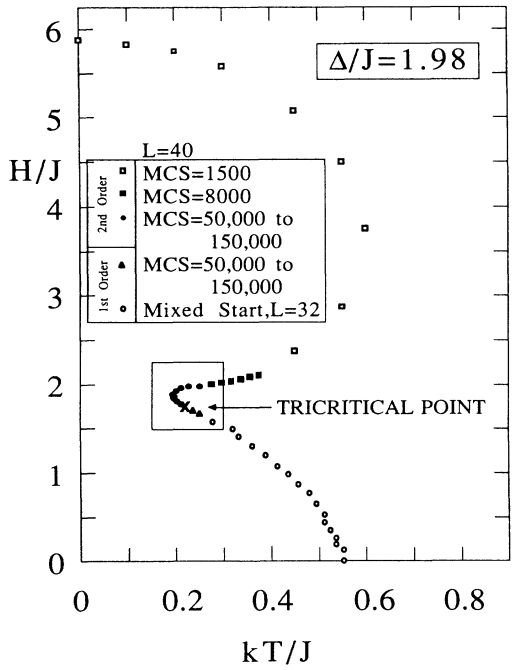

FIG. 5. Phase diagram in the $\Delta/J=1.98$ plane where the decomposition of the tricritical point might be expected. The boxed region is where measurements were concentrated.

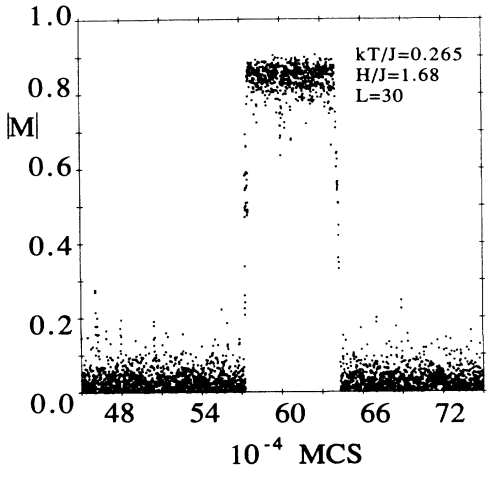

FIG. 6. Plot of the order parameter $|M|$ as a function of Monte Carlo steps. One hundred sweeps were made between plotting measurements. The presence of metastability characteristic of a first-order transition is clearly shown.

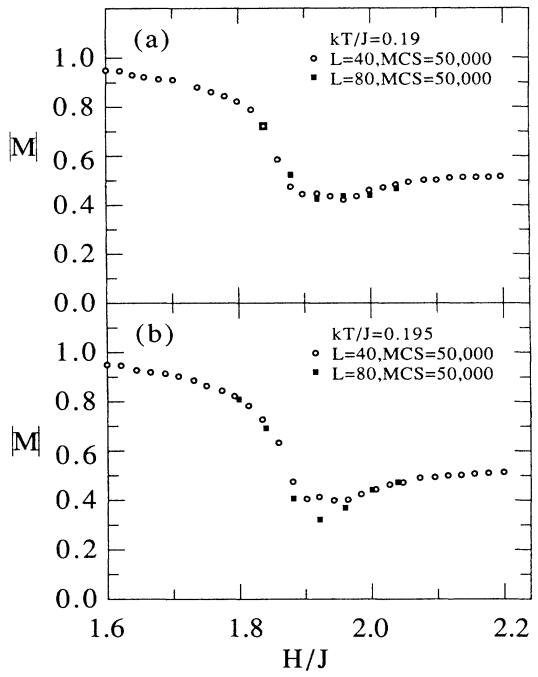

FIG. 7. Comparison of $|M|$ for $k_BT/J=0.19$ and $k_BT/J=0.195$. In (a) no evidence is seen for the lattice-size dependence expected of a second-order phase transition whereas in (b) this behavior begins to show up.

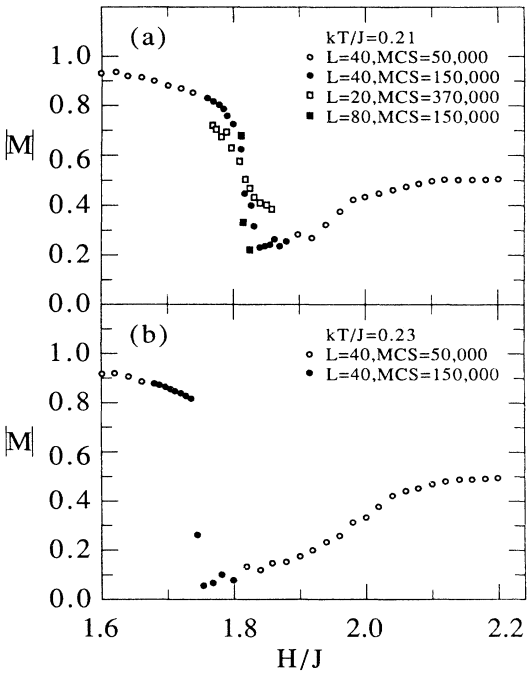

FIG. 8. Comparison of the phase transition at $k_BT/J=0.21$ and $H_c/J\simeq1.81$ which shows behavior characteristic of a second-order transition (a) with that at $k_BT/J=0.23$ and $H_c/J\simeq1.74$ which shows the discontinuity indicative of a first-order phase transition (b).

TABLE II. Determination of β near the tricritical point.

k_BT/J	H_c/J	β
0.23	2.00±0.015	0.13±0.02
0.20	1.85±0.01	0.14±0.03
0.21	1.810±0.003	0.08±0.02
0.22	1.772±0.004	0.03±0.01
0.23	1.740±0.004	0.026±0.005
0.25	1.69±0.01	0.029±0.01

gest strongly that the phase transition at $H/J=1.81$ is still second order (further evidence based on the critical index β will be presented later). However, at $k_BT/J=0.23$, the picture dramatically changes as is displayed in Fig. 8(b). Now the phase transition at $H/J\simeq1.74$ displays a definite discontinuity in $|M|$, showing that the system has passed into the region of first-order phase transition. High-statistics measurements at $k_BT/J=0.22$ indicate a behavior intermediate between that shown for the two temperatures in Fig. 8, and we conclude that the data show the point where the transition changes from second order to first order, the tricritical point, lies on the curve of Fig. 5 at $H_t/J=0.22\pm0.01$.

Further evidence for this conclusion and for our interpretation of the nature of the phase transitions in the boxed region of Fig. 5 has been obtained through an investigation of the effective critical index β in this region, determined by fitting our data to $|M|=A|(1-H_c/H)|^{\beta}$. The main source of uncertainty in the determination of β is the uncertainty in H_c. Table II summarizes our results. At $k_BT/J=0.23$ and $H_c/J=2.0$, the critical index β is equal within errors to what is expected ($\beta=0.125$) for a two-dimensional Ising second-order transition. A similar result is obtained as the measurement swings around the bend of Fig. 5 to $k_BT/J=0.2$ and $H_c/J=1.85$. However, at $k_BT/J=0.21$ the effective β begins to decline dramatically and at $k_BT/J=0.22$ is equal within errors to the tricritical index $\beta_t=0.039$ as determined by Landau and Swendsen.[5] As T is increased further, the effective β becomes even smaller as would be expected if the system has moved into a first-order transition region. These measurements, then, lead further credence to the picture exhibited in Fig. 5.

IV. SUMMARY AND CONCLUSIONS

We have made a detailed Monte Carlo study of the phase diagram and criticality of the antiferromagnetic Blume-Capel model on a two-dimensional lattice. One result is the determination of the phase diagram for this model in the three-dimensional parameter space of T, H, and Δ. Finite-size scaling and the assumption of universality was used to determine $T_c=1.694(2)$ at $H=\Delta=0$ in agreement with the low-temperature series expansion calculation[4] but with improved accuracy. The tricritical point in the $H=0$ plane has been found at a position in agreement with that determined by Landau and Swendsen[5] and the critical indices β and γ have also been found to be in agreement with those obtained in Ref. 5.

Using hysteresis measurements, we have determined the tricritical line as it evolves out of the $H=0$ plane.

Finally we have studied the question of the decomposition of the tricritical point for $H\neq 0$. No evidence is found for such a decomposition but rather we found the results shown in Fig. 5. In order to compare these results with previous work, we show in Fig. 9 the predictions of a mean-field calculation.[1] In particular Fig. 9(a) shows the tricritical point which decomposes as in Fig. 9(b) into a critical end point and a double critical point. Qualitatively there is considerable agreement between the mean-field calculation and the present Monte Carlo simulation. However, we disagree on two significant features: (i) our Monte Carlo simulation shows no evidence for the decomposition of the tricritical point and, (ii) our simulation shows that the second-order line persists around the region of high curvature in the boxed region of Fig. 5 whereas the mean-field calculation has the first-order line extending around the promontory.

We have investigated other nearby planes of fixed Δ and again find no evidence for a decomposition of the tricritical point. In regard to feature (ii), however, the difference between the mean-field calculation and the present, in principal exact simulation is readily explained. In the mean-field calculation correlated fluctuations are neglected, while for the two-dimensional lattice, fluctuations are strong in the Monte Carlo simulation. Since these fluctuations tend to break down a first-order phase transition into a second-order one, the second-order line would be expected to extend further relative to the first-order line in a calculation, such as the Monte Carlo simulation, where fluctuations are taken into account. Comparing Fig. 5 and Fig. 9 shows that it is this qualitative difference which distinguishes our result from the earlier, mean-field calculation.

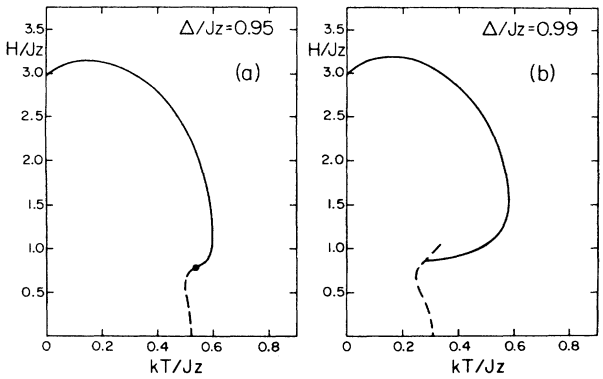

FIG. 9. Mean-field calculations from Ref. 1. Because the mean-field calculation includes in the scale the number of nearest neighbors z, one should multiply the scales of this figure by 2 to compare with Fig. 5. Solid lines represent second-order transitions and dashed lines first-order transitions. The tricritical point in (a) decomposes in (b).

ACKNOWLEDGMENTS

We wish to thank D. Duke, D. P. Landau, R. H. Swendsen, and G. Bhanot for helpful conversations, the Department of Energy and the Florida State University for providing the CYBER 205 time used in this research. The research is supported in part by The Department of Energy Grant No. DE-AS05-76ER3509) and the National Science Foundation (Grant No. DMR84-04954).

[1]Yung-Li Wang and K. Rauchwarger, Phys. Lett. **A59**, 73 (1976).
[2]H. W. Capel, Physica (Utrecht) **32**, 966 (1966).
[3]M. Blume, Phys. Rev. **141**, 517 (1966).
[4]P. F. Fox and A. J. Guttmann, J. Phys. C **3**, 913 (1973).
[5]D. P. Landau and R. H. Swendsen, Phys. Rev. Lett. **46**, 1437 (1981).
[6]N. Metropolis, A. W. Rosenbluth, M. N. Rosenbluth, A. H. Teller, and E. Teller, J. Chem. Phys. **21**, 1087 (1953).
[7]For example see D. P. Landau, Phys. Rev. B **13**, 2997 (1975).
[8]See K. Binder in *Applications of the Monte Carlo Method in Statistical Physics,* edited by K. Binder (Springer-Verlag, Berlin, 1984).
[9]M. E. Fisher, in *Proceedings of the International Summer School Enrico Fermi, Course 51, Varenna, Italy* (Academic, New York 1971); M. E. Fisher and M. N. Barber, Phys. Rev. Lett. **28**, 1516 (1972).
[10]M. N. Barber, in *Phase Transitions and Critical Phenomena,* edited by C. Domb and J. L. Lebowitz (Academic, New York, 1983), Vol. 8, p. 146.
[11]D. P. Landau, Phys. Rev. B **14**, 225 (1976).
[12]K. Binder, Thin Solid Films **20**, 367 (1974).
[13]E. Domany, K. Mon, G. V. Chester, and M. E. Fisher, Phys. Rev. B **12**, 5025 (1975).
[14]For a review see B. Hu, Phys. Rep. **91**, 233 (1982).
[15]C. Domb, Adv. Phys. **9**, 149 (1960).
[16]M. E. Fisher, Physica (Utrecht) **25**, 521 (1959).
[17]For a thorough review of the two-dimensional Ising model see B. M. McCoy and T. T. Wu, *The Two Dimensional Ising Model* (Harvard University Press, Cambridge, Mass., 1973).
[18]M. N. Barber, R. B. Pearson, D. Toussaint, and J. L. Richardson, Phys. Rev. B **32**, 1720 (1985).
[19]G. Bhanot, D. Duke, and R. Salvador, Phys. Rev. B **33**, 7841 (1986).